Journal of the European Ceramic Society 16 (1996) 421–427

0955-2219(95)00114-X
0955-2219/96/$15.00

Viscous Phase Sintering of Particle-Reinforced Glass Matrix Composites

M. Ferraris & E. Verné

Dipartimento di Scienza dei Materiali e Ingegneria Chimica, Politecnico di Torino, C.so Duca degli Abruzzi 24, I-10129 Torino, Italy

(Received 20 February 1995; revised version received 20 June 1995; accepted 28 June 1995)

Abstract

The aim of this work is the optimization of the sintering process of particle-reinforced glass matrix composites to obtain densities as close as possible to the theoretical value and improved mechanical properties in comparison with the parent glass matrix. A pressureless sintering process has been studied by means of heating-microscopy, differential scanning calorimetry and dilatometry on glass powders and mixtures of glass and reinforcement powders. The chosen glass matrix composites have the following compositions: (1) 5, 10 and 20 wt% Ti particle-reinforced ZnO–B_2O_3–PbO based glasses; and (2) 5, 10 and 20 wt% Ti particle-reinforced TiO_2–ZnO–B_2O_3–PbO based glasses. These glasses are suitable as 'model' glasses, but the method can be extended to any other matrix.

1 Introduction

Glass and glass-ceramic matrix composites (GMC, GCMC) are promising materials for structural and functional applications in the fields of automotive, aerospace and biomedical industries. They are low cost, low density, highly thermal and chemically resistant materials, compared with metal and ceramic matrix composites. The matrices are common silicate glasses or glass-ceramics, toughened by metal or ceramic fibres, platelets or particles.[1,2]

One of the main drawbacks of these materials is the difficulty in obtaining full density bodies with low cost preparation techniques (e.g. pressureless sintering). In order to focus the subject of this work, the discussion will be limited to metal particle-reinforced GMC and the optimization of a pressureless sintering process.

There are several preparation processes for GMC and GCMC materials: firstly, 'green' bodies (i.e. not sintered) can be prepared by uniaxial or isostatic cold pressing or slip casting methods. Then, there are three main sintering methods: greens can be sintered by uniaxial hot pressing or isostatic hot pressing or pressureless sintering. This last method is very attractive from an economical point of view as well as for its industrial feasibility; moreover, pressureless sintering allows the densification of larger and more complex shapes compared with expensive hot pressing or isostatic methods.

Due to the peculiarity of the glass matrix, these composites can be subjected to pressureless sintering in a viscous phase process (VPP), at temperatures well below the melting point and without any sintering aids. The key is to operate within the softening range of the glass and at the maximum temperature allowed *without any crystallization* and *with minimum viscosity*. The sintering time t is proportional to the ratio η/γ, as can be deduced from:

$$(x/a)^2 = (3/2)(\gamma/\eta)(1/a)\ t$$

where x is the neck radius between two particles, a is the particle radius, η is the viscosity and γ the surface tension of the glass, at the sintering temperature.[3–10] A pressureless method is effective when the surface tension is high and the viscosity is low, i.e. when the glass is at its lower viscosity, without any crystallization process in action.[5] If crystallization occurs, the process does not follow VPP behaviour, but other sintering theories come into play, e.g. solid or liquid phase sintering processes.

The presence of a second phase (metal particles, in this case) can interfere with the above described model: the second phase causes internal stresses in the matrix during the sintering process and the resulting sintering rate is decreased. This effect is less dramatic for the VPP of composites, because the internal stresses are almost completely absorbed by the matrix in the viscous state, but the sintering time and temperature should be *increased*

proportionally with the second phase volume fraction.[6–10] The rule of mixtures does not work above 15–20% volume fraction; above this limit, the glassy phase is not enough to guarantee a pressureless viscous phase sintering process.[6,8,11]

Furthermore, the presence of a crystalline second phase enhances the heterogeneous nucleation rate of the glass: as any crystallization during the sintering process is to be avoided,[5] the best compromise between the highest sintering rate and the lowest crystallization level needs to be determined. Moreover, by operating at the lowest possible temperature, the interfaces will be less reactive and can be designed to fulfil the composite requirements: a good interface between reinforcement and matrix is the main factor in determining the mechanical behaviour of brittle matrix composites. A subsequent heat treatment can be done to 'ceramize' the matrix and to obtain a glass-ceramic matrix composite with a low percentage of residual glassy phase.

The aim of this work is to optimize the pressureless sintering of glasses and composites with various percentages of titanium particles as the second phase, by differential scanning calorimetry (DSC) simulation of the sintering process, to find out the maximum sintering temperature, without encountering crystallization of the matrix, for both glasses and composites. To verify the effectiveness of this method a morphological and microstructural characterization was performed, and some preliminary mechanical tests were carried out on samples with a higher density, as a check on the improved mechanical properties of the composites in comparison with the parent glasses.

2 Experimental Procedure

Two glass matrices have been prepared by melting mixtures of ZnO, B_2O_3, PbO and TiO_2. The molar compositions are shown in Table 1. The addition of TiO_2 to the glass matrix modifies the interface between the titanium particles and the glass.[14,15]

The glasses have been powdered in a ball-mill and sieved to 100–140 mesh. Part of the powders were mixed with 5, 10 and 20 wt% of Ti particles (PlasmaTechnik, 99·99%) (sieved to 100 mesh). The thermal properties of the glass powders and of the mixtures of glass plus Ti were studied by means of heating microscopy (Leitz mod.II A), dilatometry (Netzsch 402) and differential scanning calorimetry (Perkin-Elmer DSC 7). The linear shrinkage versus temperature of the two glasses has been measured by heating-microscopy on cubes of pressed glass powder (heating rate 10°C min^{-1}).

Isothermal heating of the powders (glasses and glasses plus titanium) has been carried out by DSC, in the range of temperature between T_g (glass transition) and T_{x1} (first crystallization) with a 10°C min^{-1} heating rate, for 150 min under flowing Argon, in graphite crucibles. After the isothermal treatment, each sample was submitted to a scan in the temperature range 400–700°C to verify if the isothermal treatment has caused total, partial or no crystallization of the glass. The highest temperature after which the isothermally heated and scanned sample ('iso and scan' in the following text) still shows T_g and both crystallization peaks has been chosen as the maximum sintering temperature allowed for a viscous flow sintering process.

On the basis of this calorimetric study, a pressureless sintering process has been tested on greens of glass and glass plus Ti particles, under Ar flow. Greens have been prepared by uniaxial pressing, using pressures from 4 to 6 tons cm^{-2}, with the aid of liquid binders (isopropyl alcohol).

The sintered samples were characterized by X-ray diffraction (XRD, Philips PW 1710), scanning electron microscopy (SEM, Philips 525 M), compositional analysis (EDAX, Philips 9100), porosimetry (Carlo-Erba 2000 mod. 120), density measurements (Archimedean method) and mechanical tests: Young's modulus measurements (Grindosonic-Lemmens Elektronica), K_{IC} (indentation technique[16,17]) and Vickers induced crack propagation.

3 Results

Table 2 shows the characteristic temperatures (°C) and the thermal expansion coefficients (10^{-6} $°C^{-1}$) of the two glasses, obtained by DSC and dilatometry, respectively.

Figure 1 represents the percentage linear shrinkage versus temperature for ZPB (a) and TZPB (b) greens, obtained by heating microscopy. The two glasses show rapid shrinkage above 500 and 550°C, respectively, and their crystallizations occur

Table 1. Mol% composition of the two glass matrices

Sample	*ZnO*	*PbO*	*B_2O_3*	*TiO_2*
ZPB	45	15	40	—
TZPB	45	8	40	7

Table 2. Characteristic temperatures (°C) and linear expansion coefficients (10^{-6} $°C^{-1}$) of the two glasses

Sample	T_g	T_{x1}	T_{x2}	α
ZPB	479	612	653	7·96
TZPB	523	625	650	5·02

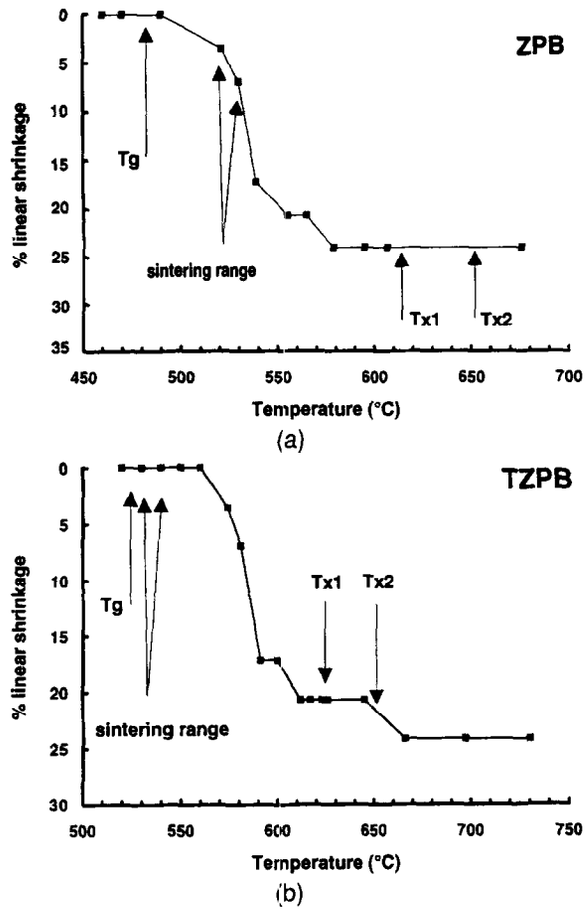

Fig. 1. Per cent linear shrinkage versus temperature for (a) ZPB and (b) TZPB greens (heating rate 10°C min^{-1}).

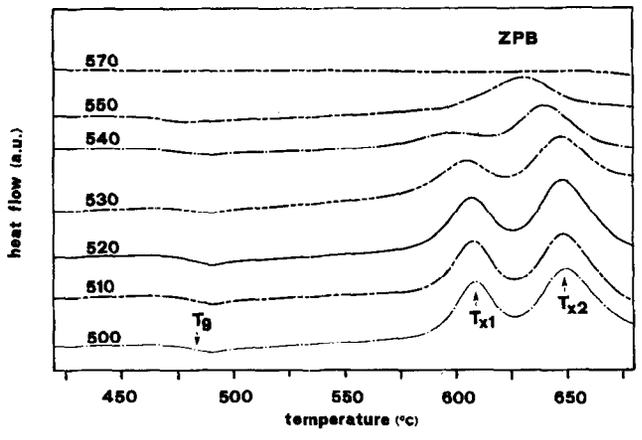

Fig. 2. DSC curves of 'iso and scan' ZPB (heating rate 10°C min^{-1}).

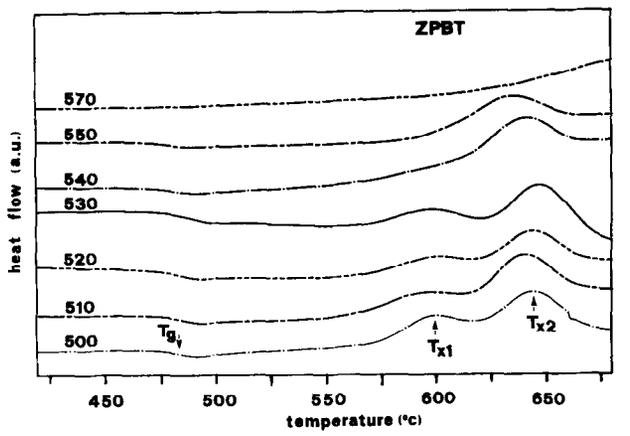

Fig. 3. DSC curves of 'iso and scan' ZPBT20 (heating rate 10°C min^{-1}).

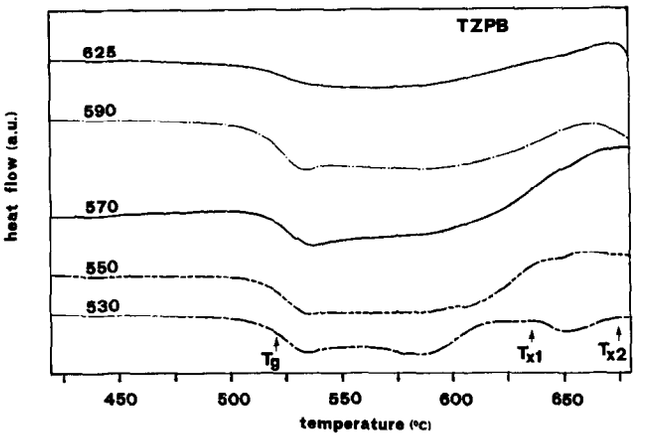

Fig. 4. DSC curves of 'iso and scan' TZPB (heating rate 10°C min^{-1}).

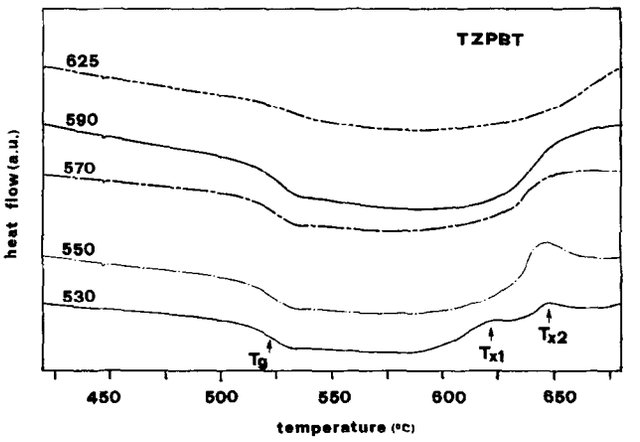

Fig. 5. DSC curves of 'iso and scan' TZPBT20 (heating rate 10°C min^{-1}).

with any volume increase. The arrows refer to the characteristic temperatures (T_g, T_{x1} and T_{x2}) obtained by DSC and to the sintering temperature chosen after DSC 'iso and scan', as described below.

Figures 2–5 show the DSC curves of ZPB (Fig. 2), ZPBT20 (ZPB powders plus 20 vol% Ti) (Fig. 3), TZPB (Fig. 4), and TZPBT20 (TZPB powders plus 20 vol% Ti) (Fig. 5): each 'iso and scan' curve represent a DSC scan made on the same powder previously heated at the temperature labelled on the curve.

The DCS scans on ZPB samples after the isothermal heatings (150 min) at 510, 520 and 530°C (Fig. 2) do not reveal any difference from the DSC of the as-prepared glass.[18] On the contrary, for the isothermal heatings at higher temperatures (from 540°C upwards), the DSC results are markedly modified: the two crystallization peaks and the T_g progressively disappear, up to the limit situation of the curve labelled 570°C, where only the melting temperature was detectable (above 700°C), which is not represented here.

Approximately the same behaviour has been found for the ZPBT20 composite (Fig. 3), where some modification of the 'iso and scan' occur from 540°C onwards.

The TiO_2 modified glass, TZPB, (Fig. 4) changes from the starting DSC 'iso and scan' curve from 550°C onwards, and the same has been found for the composite TZPBT20 (Fig. 5).

The following sintering temperature ranges have been chosen on the basis of the thermograms shown in Figs 2–5, as described above:

ZPB and ZPBT: 520–530°C
TZPB and TZBPT: 530–540°C

The composites have been sintered at temperatures about 10°C higher than the respective matrices. The per cent densities (measured density/theoretical density × 100) of the sintered glasses and composites are summarized in Tables 3 and 4. All the densities exceed 92%, with higher values for pure glasses and 5%-reinforced composites (98%) and lower values for 10- and 20%-reinforced composites.

SEM observations and porosimetric analysis confirm the density results. Figure 6 shows a polished cross-section of a ZPBT20 composite: the interfaces between Ti particles and the glass matrix are continuous and deflect a crack propagation obtained by Vickers indentation (at 5 kg; see arrows). EDS compositional results of the numbered zones are showed in Fig. 6 and its caption (1 = Ti, 2 = Pb, 3 = matrix). The values found for the glass matrix (45·4% Zn and 54·6% Pb) are in agreement with the theoretical ones (48·6% Zn and 51·4% Pb, calculated taking into account that EDS only detects metallic Zn and Pb in this glass and that the technique is semi-quantitative).

A similar behaviour pattern has been found for TZPBT composites, except for the Pb growth around Ti particles, due to a redox reaction between PbO and Ti (as described in Ref. 14).

XRD analysis on the sintered samples showed an amorphous background, with Ti and Pb signals for ZPBT composites and just Ti for TZPBT ones. The XRD instrumental detection limit is about 5% crystallinity; which means that less than 5% crystals could be present in the samples, but would not be revealed by XRD. In fact, with another kind of analysis, scanning electron microscopy (SEM), some 20%-reinforced composites revealed the presence of a few crystalline phase (approximately below 5 vol%).

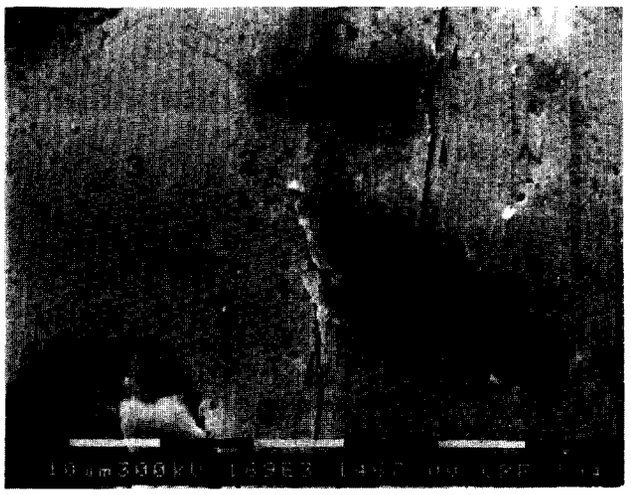

Fig. 6. SEM micrograph of ZPBT20 composite; showing induced crack propagation after Vickers indentation (1 = Ti, 2 = Pb, 3 = matrix).

The Young's moduli (E) have been measured for the as-prepared bulk glasses (70 and 80 GPa for ZPB and TZPB, respectively) and for the sintered glasses and composites having comparable densities. The obtained values for the composites are in good agreement with the theoretical ones, calculated by the following equations:[19]

$$E_c = E_m E_p/(V_m E_p + V_p E_m) \quad \text{(lower limit)}$$
$$E_c = E_m V_m + E_p V_p \quad \text{(upper limit)}$$

where: E_c = E of the composite, E_m = E of the sintered matrix, E_p = E of the Ti particles, V_m = matrix volume fraction and V_p = Ti particles volume fraction. The measured Young's modulus for the sintered ZPB is 61 GPa, and it is higher (62·5 GPa) for the corresponding composites having 5 wt% Ti particles (calculated lower and upper moduli for the composite: 62·45 and 63·37 GPa). It is 55 GPa for the sintered TZPB and 56·4 GPa for the 5 wt%-reinforced composite (calculated lower and upper moduli for the composite: 56·4 and 57·38 GPa).

Table 3. Densities of bulk and sintered glasses

Sample	*Bulk*	*Sintered*	*% Density*
ZPB	4·43	4·35	98·20
TZPB	4·02	3·94	98·34

Table 4. Theoretical and experimental densities of sintered samples

Sample	*ZPBT*			*TZPBT*		
Wt% Ti	5	10	20	5	10	20
Theoretical density (g cm^{-3})	4·43	4·44	4·44	4·04	4·07	4·12
Measured density (g cm^{-3})	4·35	4·29	4·09	3·99	3·87	3·85
% Densities	98·2	96·9	92·2	98·8	95·1	93·4

The K_{IC} values (calculated as reported in Refs 16 and 17) for the sintered glasses are, respectively; 0·574 MPa $m^{1/2}$ (ZPB) and 0·578 MPa $m^{1/2}$ (TZPB). The K_{IC} value for the 5 wt%-reinforced TZPBT composite is about twice the matrix one: 1.027 MPa $m^{1/2}$.

4 Discussion

The ZPB glass matrix is a typical non-silica based 'soft' glass,[12,13] chosen in this work for its low characteristic temperatures suitable for a DSC based study; the glass composition has been modified by adding 7 mol% TiO_2 to change the interfacial reactivity between the matrix and Ti particles in the composites, as discussed in a previous paper[14] and in Ref. 15. The aim of this work is to find the suitable temperature range for a viscous-phase pressureless sintering process for glasses and composites: crystallization of the samples during sintering is to be avoided, otherwise the sintering temperatures should be increased and a certain pressure required to obtain full density; furthermore, the crystalline phases could have different expansion coefficients with respect to the matrix and cause cracks or voids in the sintered sample.

The first useful information about the sintering behaviour is given by the per cent linear shrinkage versus temperature (Figs 1(a) and (b)): ZPB and TZPB could be sintered from 575 and 650°C onwards, respectively (maximum value of % shrinkage). This information, the same as is obtainable by dilatometric studies, must be completed, for glasses, with other considerations: as indicated by the arrows, 575 and 650°C are very close to or above the crystallization temperatures (T_{x1} and T_{x2}). As the sintering process requires isothermal treatment of the sample at these temperatures, it must be pointed out that the sample will not be in the glassy state during the entire process, but is transformed to a partially or totally crystallized sample during the process. It must also be pointed out that a glass of the same system (ZnO–PbO–B_2O_3) starts with homogeneous surface crystallization after 1 h at 420°C.[12] The linear shrinkage versus temperature gives us initial rough information about the sintering behaviour, but it is not representative of the actual sintering process. In particular, it does not take into account the kinetics of crystallization: the maximum shrinkage temperature recorded with a heating rate of about 10°C min^{-1} can not be immediately transferred to a sintering process which requires a prolonged isothermal step. During this time the sample could partially or totally crystallize. A more realistic way to simulate the sintering process could be to consider several isothermal heatings at different temperatures inside the heating-microscope, but the choice of temperatures could require several time-consuming experimental runs.

The alternative way proposed in this work takes into account the high sensitivity of the DSC in detecting glass transition and crystallization in glasses: the 'iso and scan' method is more representative of the sintering process than a heating-microscopy or dilatometric study, it does not require the preparation of greens and it is very attractive from an experimental (runs versus time) point of view.

In order to know exactly if the sample is still amorphous or crystalline after an isothermal heating, the 'iso and scan' curves of Figs 2–5 are of immediate utility: if the 'iso and scan' curve shows any modification from the previous one, it means that something is happened during the isothermal heating at that temperature, so that temperature may be too high to sinter in a pure glassy state. This method also takes into account the nucleating effect of TiO_2 and of Ti particles in composites: in these cases, suitable temperatures to work in the glassy state must be lowered, because crystallization is favoured by the presence of these substances.

The nucleating effect of TiO_2 can be noted by comparing Figs 2 and 4 (ZPB and TZPB 'iso and scan' curves, respectively): the stability of the titania-containing glass matrix is decreased by ~100°C ($T_{x1} - T_g$). By comparing Figs 2 and 3 (ZPB and ZPBT 'iso and scan' curves, respectively), the nucleating effect of Ti can be noted by the decreasing crystallization onset in the composite with respect to the pure glass matrix. The same is true for Figs 4 and 5 (TZPB and TZPBT 'iso and scan' curves, respectively). Titanium particles also have an opposite effect: the sintering temperature of the composites must be increased with respect to the matrix one, proportionally to the volume fraction of the second phase.[3–8]

The 'iso and scan' curves gave an immediate answer to sample modification (with or without a different percentage of second phase) during the sintering process. Figures 2–5 show the two extremes of behaviour (pure glass matrices and 20% Ti composites, the 5 and 10% Ti composites being similar to the former and latter case, respectively).

The chosen sintering temperature ranges, indicated by arrows in Figs 1(a) and (b) for ZPB and TZPB glasses, respectively, stress the above discussed differences between heating-microscopy and DSC study of the process: ZPB glass starts to sinter at 520–530°C, but it reaches its constant shrinkage values after 575°C. 'Iso and scan' curves for ZPB (Fig. 2) show that already, after an

isothermal heating at 530°C, the sample starts to show modifications from the glassy state. In fact, a pressureless sintering process at 520°C gave 98·20% density (Table 3), whereas higher sintering temperatures gave lower density values. Even more dramatic is the kinetic factor for TZPB (Fig. 1(b)) where, apparently, the DSC derived sintering range (530–540°C) is below the shrinkage curve slope onset temperature. In this particular case, the presence of a nucleating agent such as titania causes an early nucleation and crystallization during the isothermal heating of the glass, well below the recorded crystallization temperature onset! In this last case, as well as for the composites, the 'iso and scan' method revealed its effectiveness: TZPB sintered at 530°C showed the maximum density obtained (98·34%) (Table 3).

For the composites, the two opposite effects of Ti particles (the sintering temperature for the glassy state must be decreased because of its nucleating effect, but also increased because of its second phase effect) are clearly evident in Table 4: the 'iso and scan' method proved to be effective for 5 and 10% Ti composites, but fails at 20%. In this last case, 92–93% density is the maximum value obtainable by pressureless sintering in the glassy state: by increasing the sintering time or temperature, a partial crystallization of the samples has been observed. The process is not a VPP and the use of pressure could be useful to obtain a full density vitreous composite.

Obtaining high density composites allows their mechanical characterization, in order to verify their improved mechanical properties with respect to the matrix. Figure 6 shows a polished cross-section of a ZPBT composite (20% Ti): the Vickers induced crack (see arrows) is made to deviate by Ti particles (bridging). This energy-consuming mechanism is responsible for composite toughening, compared with the sintered glass matrix. In fact, the measured Young's moduli, as well as the calculated K_{IC} values, are higher for composites than for pure matrices, confirming that the interfaces between the matrix and reinforcements are continuous and act as a load transfer zone between the brittle matrix and ductile particles, leading to toughening of the material.

5 Conclusions

These first results let us show that pressureless sintering of glass matrix composites must occur in the glassy state; the sintering temperature must be chosen as high as possible to minimize the viscosity and the sintering time, *always being in the glassy state*. If any crystallization begins, the viscosity of the system abruptly increases, and the sintering time and temperature must be prolonged and the use of hot-pressing techniques could be required to obtain fully densified samples. Furthermore, the use of higher temperatures is normally considered detrimental for interfacial reactivity and consequently for the mechanical properties of the composites (i.e. the formation of thick reaction layers between particles and matrix could occur).

The 'iso and scan' curves are an effective method to identify a sintering temperature range in the glassy state, taking into account some fundamental factors such as the decreasing sintering rate, and the nucleation effect of the reinforcement, as well as the kinetic contribution occurring during the sintering process.

Acknowledgements

The authors wish to thank Dr. P. Lemoine and Professor M. Montorsi for their remarkable scientific contribution and friendly collaboration, and FIAT Research Centre (CRF — Orbassano, Torino) for the SEM–EDS facilities.

References

1. Bleay, S. M. & Scott, V. D., Microstructure and micromechanics of the interface in carbon fibre reinforced Pyrex glass. *J. Mater. Sci.*, **26** (1991) 3544–52.
2. Hegeler, H. & Brueckner, R., Mechanical properties of carbon fibre-reinforced glasses. *J. Mater. Sci.*, **27** (1992) 1901–7.
3. Pastor, H., La cinetique du frittage sous pression. *Rev. Int. Hautes Temp. et Réfract.* (1972) 251–64.
4. Exner, H. E. & Petzow, G., Shrinkage and rearrangement during sintering of glass spheres. In *Sintering and Related Phenomena, Materials Science Research*, ed. Kuczynski. Plenum Press, New York, 1973, Vol. 6, pp. 279–93.
5. Panda, P. C. & Raj, R., Sintering and crystallization of glass at constant heating rate. *J. Am. Ceram. Soc.*, **72**(8) (1989) 1564–6.
6. Bordia, R. & Raj, R., Analysis of sintering of composite with glass or ceramic matrix. *J. Am Ceram. Soc.*, **69**(3) (1989) C55–7.
7. Scherer, G. S., Sintering with rigid inclusions. *J. Am. Ceram. Soc.*, **70**(10) (1987) 719–25.
8. Rahaman, M. N. & De Jonghe, L. C., Effect of rigid inclusions on the sintering of glass powder compacts. *J. Am. Ceram. Soc.*, **70**(12) (1987) C348–51.
9. Jean, J. H. & Gupta, T. K., Liquid-phase sintering in the glass–cordierite system. *J. Mater. Sci.*, **27** (1992) 1575–84.
10. Fan, C. L. & Rahaman, M. N., Factors controlling the sintering of ceramic particulate composites: I. conventional processing. *J Am. Ceram. Soc.*, **75**(8) (1992) 2056–65.
11. Dutton, R. E. & Rahaman, M. N., Sintering, creep, and electrical conductivity of model glass-matrix composites, *J. Am. Ceram. Soc.*, **75**(8) (1992) 2146–54.
12. Shinkai, N. R., Bradt, C. & Rindone, G. E., Elastic modulus and fracture toughness of ternary $PbO–B_2O_3–ZnO$ glasses. *J. Am. Ceram. Soc.*, **65**(2) (1982) 123–6.
13. Rabinovich, E. R., Crystallization and thermal expansion

of solder glass in the $PbO–B_2O_3–ZnO$ system with admixtures. *Ceram. Bull.*, **58**(6) (1969) 595–8.
14. Ferraris, M., Badini, C. & Couzinet, B., Interfacial equilibria in titanium particle/glass ceramic composites. *Composites*, **25**(7) (1994) 494–8.
15. Donald, I. W., Preparation, properties and chemistry of glass- and glass-ceramic-to-metal seals and coatings. *J. Mater. Sci.*, **28** (1993) 2841–86.
16. Anstis, G. R., Chantikul, P., Lawn, B. R. & Marshall, D.B., A critical evaluation of indentation techniques for measuring fracture toughness: I, direct crack measurements. *J. Am. Ceram. Soc.*, **64**(9) (1981) 533–8.
17. Breder, K., Zeng, K. & Rowcliffe, D. J., Indentation testing of an Al_2O_3/SiC whisker composite. *Ceram. Eng. Sci. Proc.*, **10**(7–8) (1989) 1005–13.
18. Montorsi, M., Ferraris, M., Verné, E. & Lemoine P., Sintering of glass-ceramic matrix composites: an approach to the process optimisation. In *Proceedings of The 1995 IChemE Research Event*, ed. by the Institution of Chemical Engineers, Warwickshire, 1995, pp. 814–16.
19. Callister, W. D. Jr, *Materials Science and Engineering, an Introduction*. John Wiley & Sons, New York, 1990.